Title

Rotaxane Probes for the Detection of Hydrogen Peroxide by 129Xe HyperCEST NMR Spectroscopy

Journal

Angewandte Chemie International Edition, 58(29)

ISSN

1433-7851

Authors

Klass, Sarah H

Truxal, Ashley E

Fiala, Tahoe A

et al.

Publication Date

2019-07-15

DOI

10.1002/anie.201903045

COMMUNICATION

Rotaxane probes for the detection of hydrogen peroxide by ^{129}Xe hyperCEST NMR

Sarah H. Klass,[a] Ashley E. Truxal,[a] Tahoe A. Fiala,[a] Joseph Kelly,[a] Dang Nguyen,[a] Joel Finbloom,[a] David E. Wemmer,[a] Alexander Pines,[a,b] Matthew B. Francis [a,b,*]

[a]*Department of Chemistry, University of California, Berkeley, and* [b]*Materials Sciences Division, Lawrence Berkeley National Laboratories, Berkeley, California 94720.*

**mbfrancis@berkeley.edu*

Abstract: The development of sensitive and chemically selective MRI contrast agents is imperative for the early detection and diagnosis of many diseases. Conventional responsive contrast agents used in ^{1}H MRI are impaired by the high abundance of protons in the body. ^{129}Xe hyperCEST NMR/MRI comprises a highly sensitive complement to traditional ^{1}H MRI due to its ability to report specific chemical environments. To date, the scope of responsive ^{129}Xe NMR contrast agents lacks breadth in the specific detection of small molecules, which are often important markers of disease. Herein, we report the synthesis and characterization of a rotaxane-based ^{129}Xe hyperCEST NMR contrast agent that can be turned on in response to H_2O_2, which is upregulated as a result several disease states. Added H_2O_2 was detected by ^{129}Xe hyperCEST NMR in the low μM range, as well as H_2O_2 produced by HEK 293T cells activated with tumor necrosis factor.

The sensitive and selective detection of disease markers is of high importance for the identification and treatment of a variety of human diseases. Magnetic resonance imaging (MRI), the clinical version of nuclear magnetic resonance (NMR) spectroscopy, is a noninvasive imaging technique that can achieve high resolution and excellent tissue penetration. Conventional MRI techniques rely on differences in the relaxation properties of protons primarily associated with water molecules in different tissue types. Typically, contrast agents in the form of paramagnetic metal chelates or spin-labeled biomolecules alter the relaxation properties of local water molecules to provide additional structural and functional information.[1] Responsive ^{1}H and ^{13}C NMR contrast agents have also been developed that produce a signal only in the presence of particular disease markers, such as enzymes, signaling molecules, and oxidizing conditions.[2,3,4,5] This approach can aid in early disease detection and provides insight into the chemical environment, ultimately enabling a better understanding of disease pathology. However, even with these contrast agents, signal and sensitivity are often lost due to spectral complexity within the limited chemical shift range that protons possess.

Hyperpolarized xenon chemical exchange saturation transfer (^{129}Xe hyperCEST) NMR comprises a sensitive complement to traditional ^{1}H MR imaging approaches.[6] Although it is a non-toxic and non-reactive noble gas, xenon is very sensitive to its local chemical environment due to its high electron polarizability. The easy deformation of its electron cloud leads to chemical shifts that range over several hundred ppm in biological samples, enabling direct and quantitative imaging of local spin environments that are often indistinguishable via conventional MRI.[7] The combination of this acute sensitivity and xenon's high solubility in blood, tissue, and lipophilic membranes distinguishes it from other heteronuclear contrast agents.[8] Further, facile hyperpolarization of ^{129}Xe nuclei can be obtained through spin exchange optical pumping, leading to contrast enhancements of 4-5 orders of magnitude over thermal polarization.[9] The lack of background ^{129}Xe signals in most systems gives rise to uncomplicated spectra as well as the potential for improved resolution of small, localized populations of target molecules.[10]

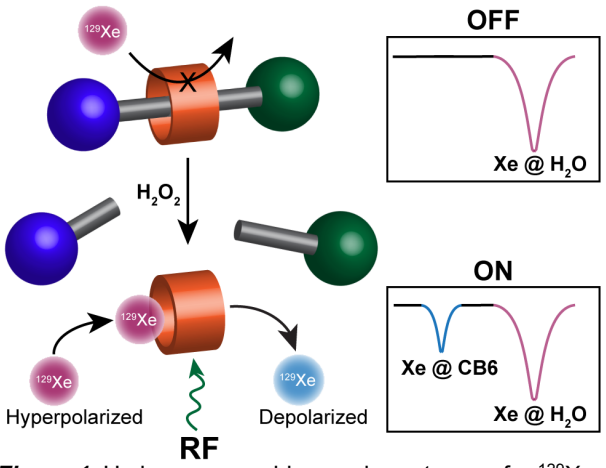

Figure 1. Hydrogen peroxide-sensing rotaxane for ^{129}Xe hyperCEST NMR. CB6 (orange) is threaded along a molecular axle (gray) that is mechanically locked into place by the presence of two bulky stoppers (blue and green), creating a supramolecular complex known as a rotaxane. The presence of the axle in the interior of CB6 prevents Xe from entering the cavity and thus presents no Xe@CB6 signal in the hyperCEST NMR spectrum (OFF). After cleavage of one of the bulky stoppers by a reaction with H_2O_2, the CB6 cavity becomes available to form a host-guest complex with Xe atoms. Insets: When inside the CB6 cavity, the Xe experiences a relatively shielded environment, creating a unique chemical shift observable by Xe NMR. An RF saturation pulse corresponding to this chemical shift can be applied to depolarize the Xe selectively inside the CB6. The reduction of the bulk hyperpolarized Xe (Xe@H_2O) signal as a result of depolarizing xenon at the Xe@CB6 chemical shift is then observed (ON). Recording the Xe@H_2O signals using an array of saturation frequencies yields the above z-spectra.

Being chemically inert, ^{129}Xe is effectively functionalized for selective detection by participating in supramolecular host-guest interactions that cause either large chemical shifts or changes in relaxation parameters that are distinct to the host environments in which ^{129}Xe resides.[11,12,13,7] Since the majority of xenon atoms are present in bulk solution and undergo continuous exchange with host molecules, we can exploit the exchange between host-bound and "free" xenon by way of CEST techniques to attain detection limits of hosts down to sub-nM levels.[14,15]

To create "turn-on" ^{129}Xe hyperCEST NMR contrast agents, researchers have used the known Xe host cucurbit[6]uril (CB6) due to its favorable exchange parameters for hyperCEST applications.[15,16] CB6 is a toroidal molecule that can harbor a single ^{129}Xe atom in its interior cavity, creating a distinct ^{129}Xe@CB6 chemical shift.[17] CB6 has been used as an *in vivo* contrast agent in rat vasculature, highlighting the applicability of future designs based on this moiety.[18] To prevent ^{129}Xe molecules from entering the interior of CB6 and producing this unique signal until desired, the CB6 can be threaded onto a molecular axle. This axle is then capped by two bulky stopper groups, creating the supramolecular species known as a rotaxane.[19,20] By designing one of these bulky stoppers to be cleaved under specific conditions, such as activation by a disease marker, a Xe@CB6 signal can be selectively observed only when activated. Using these design principles, our group and others have previously produced rotaxanes and rotaxane-like species where the CB6 response is occluded by a molecular species threaded through the cavity. These systems have been designed to release CB6 under a variety of conditions, such as strong base,[14] cancer-related matrix-metalloproteinase (MMP) enzymes,[21] and the human carbonic anhydrase enzyme.[22] This "turn on" effect differs in concept from other systems, such as the previously reported biotinylated CB7 construct, which exhibits a unique NMR shift upon binding to its protein target.[23] In other work, cyclodextrin based pseudorotaxanes have also provided encouraging results.[24]

Based on the design elements of these first examples, we sought to create a probe that would be responsive to increased levels of hydrogen peroxide (H_2O_2, Figure 1). Prior research has implicated upregulated levels of H_2O_2 production in the advancement of inflammation, and increases in oxidative stress have been correlated with the

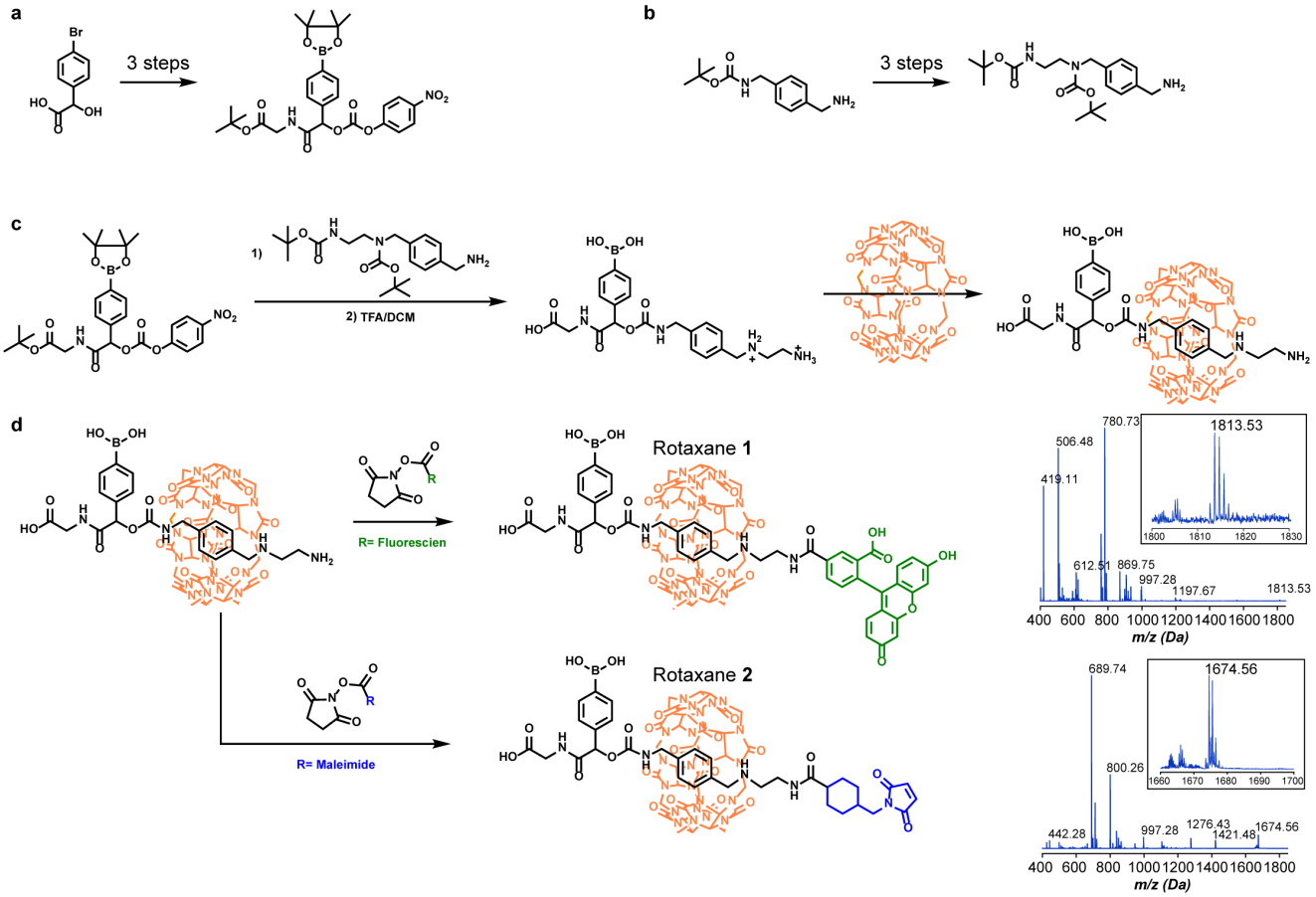

Figure 2. Convergent synthesis of Rotaxane 1 and Rotaxane 2. (a) The synthetic route to produce a H_2O_2 sensing cap involved three steps, and (b) the synthetic route to produce a paraxylene diamine axle required four steps. (c) The two segments were combined using a 2-step procedure and subsequently threaded with CB6. (d) The axles were then capped with either fluorophore or maleimide functionalities resulting in the formation of Rotaxane 1 and Rotaxane 2 respectively. LC-MS traces are shown for Rotaxane 1 (expected m/z: 1813.44; observed m/z: 1813.53, boron isotope pattern observed) and Rotaxane 2 (expected m/z: 1674.37; observed m/z: 1674.56, boron isotope pattern observed).

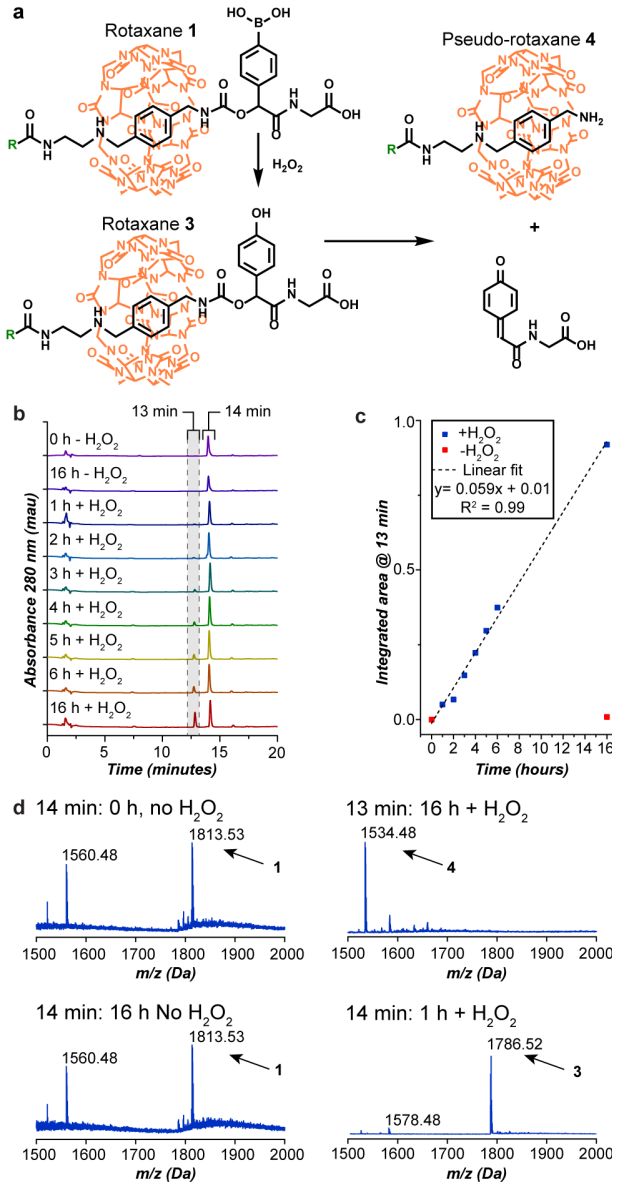

Figure 3. HPLC and ESI-TOF MS analysis of rotaxane cleavage by H_2O_2. (a) The method of cleavage by H_2O_2 is shown for Rotaxane 1. (b) HPLC analyses followed the absorbance over the course of 16 h. A control sample with no H_2O_2 added was used to determine if any degradation of the rotaxane occurred. Starting Rotaxane 1 and oxidized Rotaxane 3 both eluted at 14 min, but could be distinguished using ESI-TOF MS. The peak that emerges at 13 min was identified as cleaved pseudo-rotaxane product 4. (c) Integration of the peak area at 13 min afforded a linear relationship with respect to time. (d) MS analysis of peak at 13 min is shown: expected m/z: 1534.43; observed m/z: 1534.48. MS analysis of peak at 14 min corresponded to the intact rotaxane, with the boronic acid group present only in samples that had not been exposed to H_2O_2 (0 and 16 h time points). In all samples that had been exposed to H_2O_2 the MS trace corresponded solely to the oxidized phenol rotaxane (expected m/z: 1785.62; observed m/z: 1786.52).

advancement of cancer[25], diabetes[26], cardiovascular disease, pulmonary disease, and wound healing.[27,28] The high sensitivity of ^{129}Xe hyperCEST NMR could allow for the detection of extracellular H_2O_2 at the low physiological levels (0.5-50 μM) associated with these disease states.[29,27]

^{129}Xe MRI has demonstrated a unique strength in functional lung imaging, making oxidatively sensitive sensors most provocative for the detection of pulmonary afflictions in which abnormally increased levels of H_2O_2 have been linked. Known examples include chronic obstructive pulmonary disease, community-acquired pneumonia, cancer of the lung, and denervation-induced muscle atrophy.[18,19,20] Current examples for imaging H_2O_2 *in vivo* or in opaque environments include chemiluminescent nanoparticles, a ^{13}C-labeled MRI probe, and a bioluminescent reporter.[4,33,34] However, these techniques suffer from either limited sensitivity or the requirement of modifying the natural sample environment. Therefore, imaging H_2O_2 in an unperturbed environment at physiologically relevant concentrations remains an interesting challenge. Herein we describe the first synthesis, characterization, and application of a ^{129}Xe hyperCEST contrast agent for the detection of H_2O_2.

Several design elements were considered in the synthesis of a rotaxane that could function as a ^{129}Xe hyperCEST turn-on probe in response to H_2O_2: (1) Inspired by the design of several H_2O_2 activated fluorescent, positron emission tomography (PET), and ^{1}H/^{13}C MRI probes, we incorporated a sensitive and selective aryl boronic acid group as a cleavable cap on the rotaxane (Figure 2a);[34,35,36,37,29] (2) To improve sensitivity, the rotaxane axle was composed of a *p*-xylene diamine moiety that has one of the lowest reported K_a values for CB6 (5.5 x10^2 M^{-1}, Figure 2b);[19] (3) To allow for ease of synthesis and modification to the rotaxane design, a convergent route was designed, in which the axle and cap were joined at later steps (Figure 2c). Using this route, two such rotaxanes were prepared with differing non-responsive capping moieties. Rotaxane **1** was capped with a fluorophore to allow for specific UV detection during HPLC/LC-MS cleavage studies (Figure 2d). Rotaxane **2** was capped with a maleimide functional group that allows for further conjugation to biomolecules and was used in the ^{129}Xe hyperCEST experiments (Figure 2e). Both molecules were purified using RP-HPLC before use.

To determine the cleavage rates of the rotaxane caps in the presence of excess H_2O_2, a sample of Rotaxane **1** was monitored over time by HPLC/LC-MS. Rotaxane **1** was found to be completely oxidized within 1 h. However, the 1,6 elimination reaction that ultimately results in bond cleavage proved to be the slow step, with less than 50% cleavage after 16 h. Kinetic measurements extrapolated from these data (assuming pseudo-first-order conditions with 7.5 μM Rotaxane **1** and 100 μM H_2O_2 in 1xPBS buffer at pH 7.4) gave a rate constant of k= 8.52 x 10^{-3} s^{-1} (Figure 3).

To determine if the sucessful cleavage reaction observed using LC-MS resulted in a ^{129}Xe hyperCEST signal, multiple concentrations of Rotaxane **2** and H_2O_2 were analyzed to monitor the emergence of the Xe@CB6 signal over time. A Xe@CB6 hyperCEST response evolved within 1 h following

the addition of 2 equivalents of hydrogen peroxide (25 μM Rotaxane **2**, 50 μM H_2O_2) , and quickly reached and maintained an apparent maximum saturation of about 25% (Figure 4a). Previous rotaxane-based sensors have required 8-24 h to demonstrate the same magnitude of CEST response, demonstrating the notable improvement in efficiency and sensitivity of this system.[14,21] Evaluation of Rotaxane **2** (Figure 4b) and H_2O_2 at varying concentrations (Figure 4c) led to detection limits of 2.5 μM and 5 μM, respectively. Notably, the limits of detection could be significantly improved by new advancements in hyperpolarization methods, where ^{129}Xe hyperpolarization levels of greater than 50% have been obtained.[38] This is a large enhancement over the polarization levels used in this study, which were only 0.05-2%.

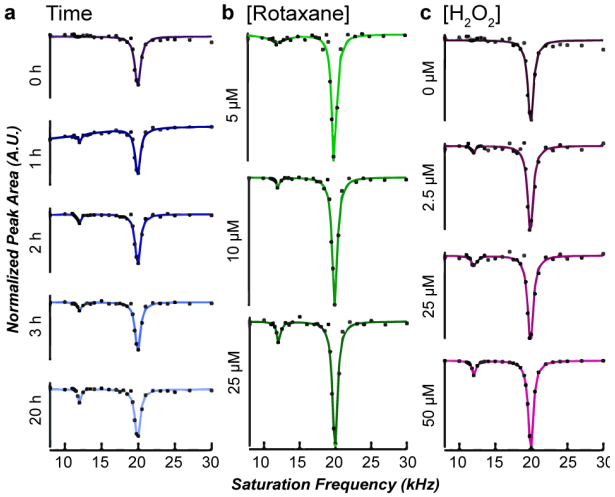

Figure 4. Rotaxane 2 acts as a ^{129}Xe hyperCEST NMR probe for H_2O_2. (a)The signal at 20 kHz corresponds to bulk dissolved xenon in water and is always present, but upon addition of H_2O_2, cleavage of Rotaxane 2 releases CB6. This leads to the immediate appearance of a Xe@CB6 CEST response at 12 kHz that builds over time. (b,c) The signal can be observed down to 5 μM Rotaxane 2 and 2.5 μM H_2O_2.

Although the observed response magnitudes did increase with increasing Rotaxane **2** or H_2O_2 concentration, they did not seem to be able to achieve more than 25-28% saturation. In contrast, a 5 μM solution of free CB6 that was not previously threaded onto a rotaxane provided nearly complete saturation immediately using the same acquisition parameters. One explanation for the incomplete saturation could be the formation of a complex between the carbonyl-rich portal of CB6 and the protonated amine remaining at the end of the cleaved rotaxane. CB6 is known to form such complexes with short peptides as well as long diammonium alkanes.[39,40,41] This includes the *p*-xylylene diamine group used in this study.[19] Indeed, we can observe an intact CB6•4 complex by HPLC/LCMS after axle cleavage by H_2O_2. Furthermore, the mass spectra indicate that H_2O_2 does not affect the molecular structure of the CB6 or the cleaved axle. Presumably the interaction with the cleaved axle sequesters some of the CB6, thus limiting the saturation level that is observed. Nonetheless, the successful acquisition of a Xe@CB6 response indicates that enough CB6 is released for xenon exchange into and out of the cavity.

The maleimide cap on Rotaxane **2** enabled the functionalization of cysteine residues present on the vascular cell adhesion molecule (VCAM)-1 binding peptide and a tobacco mosaic virus (TMV) protein-based nanoparticle. The VCAM-1 binding peptide was chosen because this receptor has implications in inflammatory disease and cancer.[42,43] TMV is a disk shaped nanoparticle that assembles into a nanoscale structure that is 17 nm in diameter and composed of 34 protein monomers.[44] This protein assembly was chosen for is distinct morphology, which could be adventageous in drug delivery and imaging applications.[45,46] Using excess Rotaxane **2**, the VCAM-1 peptide was completly modified, while the TMV nanoparticle was purposefully modified at 30% of its available sites, resulting in 10 rotaxane molecules per TMV disk (Figure S1).

We then sought to detect endogenously produced H_2O_2 by exposing HEK 293T cells to tumor necrosis factor alpha (TNF), a signaling protein involved in immune cell regulation that causes an increase in cellular H_2O_2 production.[47,48] Adherent cells in 6 well plates were either exposed to 40 μg of TNF (TNF+) or remained untreated (TNF–). Both samples were incubated for 6 h at 37 °C under an atmosphere of 5%

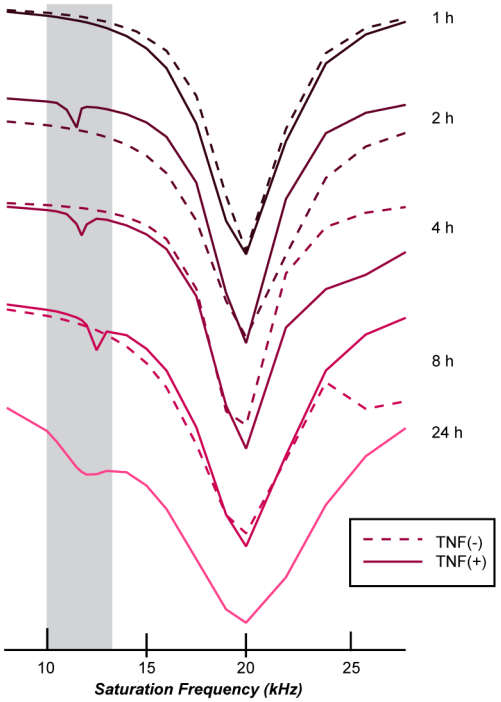

Figure 5. Detection of a ^{129}Xe hyperCEST signal in response to endogenously produced H_2O_2. TMV-Rotaxane 2 was added to the supernatants from HEK 293T cells with (TNF+) or lacking (TNF–) TNF in the cultures. The samples were monitored for a Xe@CB6 CEST response over 24 h. No Xe@CB6 response appeared for the any of the TNF(–) samples, while a signal at 10-13 kHz appeared and stabilized within a few hours for the TNF+ samples.

CO_2. The supernatant was then treated with the TMV-Rotaxane **2** conjugate to a final concentration of 1 μM (corresponding to 10 μM Rotaxane **2** groups). The samples were examined by ^{129}Xe hyperCEST NMR over the course of several hours (Figure 5). No Xe@CB6 signal evolved for the TNF– sample, even after 8 h. In contrast, a response evolved and stabilized after 2 h for the TNF+ sample. The Xe@CB6 signal, albeit significantly broadened, persisted even after 24 h. By comparison with the experiment in which exogenous H_2O_2 was added to HEK 293T cells, we estimate low μM H_2O_2 was expressed as a result of incubation with TNF. This is well within the detection limit of both sensor and target, demonstrating the utility of this technique to detect biologically relevant concentrations.

In conclusion, we have demonstrated the synthesis of a novel CB6 rotaxane that enables the selective detection of endogenously produced H_2O_2 by ^{129}Xe hyperCEST NMR. These results provide an important foundation for future applications focusing on the diagnostic imaging of diseased tissue in which peroxide levels are abnormally increased.

Experimental Section

Full experimental methods can be found in the Supporting Information.

Acknowledgements

This work was supported by the UCSF Hana Jabsheh Fund. S.H.K. was supported by the Chemical Biology Graduate Program at UC Berkeley (NIH T32-GM066698). J.A.F. was supported under contract FA9550-11-C-0028 and awarded by the Department of Defense, Air Force Office of Scientific Research, National Defense Science and Engineering Graduate (NDSEG) Fellowship, 32 CFR 168a.

Keywords:
Rotaxanes
^{129}Xe hyperCEST NMR
NMR spectroscopy
CB6: Cucurbit[6]uril

References

(1) Caravan, P. Strategies for Increasing the Sensitivity of Gadolinium Based MRI Contrast Agents. *Chem. Soc. Rev.* **2006**, *35* (6), 512.

(2) Park, J. Y.; Baek, M. J.; Choi, E. S.; Woo, S.; Kim, J. H.; Kim, T. J.; Jung, J. C.; Chae, K. S.; Chang, Y.; Lee, G. H. Paramagnetic Ultrasmall Gadolinium Oxide Nanoparticles as Advanced T_1 MRI Contrast Agent: Account for Large Longitudinal Relaxivity, Optimal Particle Diameter, and *In Vivo* T_1 MR Images. *ACS Nano* **2009**, *3* (11), 3663–3669.

(3) Ye, D.; Shuhendler, A. J.; Pandit, P.; Brewer, K. D.; Tee, S. S.; Cui, L.; Tikhomirov, G.; Rutt, B.; Rao, J. Caspase-Responsive Smart Gadolinium-Based Contrast Agent for Magnetic Resonance Imaging of Drug-Induced Apoptosis. *Chem. Sci.* **2014**, *5* (10), 3845.

(4) Lippert, A. R.; Keshari, K. R.; Kurhanewicz, J.; Chang, C. J. A Hydrogen Peroxide-Responsive Hyperpolarized ^{13}C MRI Contrast Agent. *J. Am. Chem. Soc.* **2011**, *133* (11), 3776–3779.

(5) Angelovski, G.; Gottschalk, S.; Milošević, M.; Engelmann, J.; Hagberg, G. E.; Kadjane, P.; Andjus, P.; Logothetis, N. K. Investigation of a Calcium-Responsive Contrast Agent in Cellular Model Systems: Feasibility for Use as a Smart Molecular Probe in Functional MRI. *ACS Chem. Neurosci.* **2014**, *5* (5), 360–369.

(6) Witte, C.; Kunth, M.; Döpfert, J.; Rossella, F.; Schröder, L. Hyperpolarized Xenon for NMR and MRI Applications. *J. Vis. Exp.* **2012**, No. 67.

(7) Wang, Y.; Dmochowski, I. J. An Expanded Palette of Xenon-129 NMR Biosensors. *Acc. Chem. Res.* **2016**, *49* (10), 2179–2187.

(8) Mcmahan, Z. H.; Wigley, F. M. *HHS Public Access*; 2015; Vol. 5.

(9) Walker, T. G.; Happer, W. Spin-Exchange Optical Pumping of Noble-Gas Nuclei. *Rev. Mod. Phys.* **1997**, *69* (2), 629–642.

(10) Oros, A. M.; Shah, N. J. Hyperpolarized Xenon in NMR and MRI. *Phys. Med. Biol.* **2004**, *49* (20).

(11) Bartik, K.; Luhmer, M.; Dutasta, J.-P.; Collet, A.; Reisse, J. 129 Xe and 1 H NMR Study of the Reversible Trapping of Xenon by Cryptophane-A in Organic Solution. *J. Am. Chem. Soc.* **1998**, *120* (4), 784–791.

(12) Spence, M. M.; Rubin, S. M.; Dimitrov, I. E.; Ruiz, E. J.; Wemmer, D. E.; Pines, A.; Yao, S. Q.; Tian, F.; Schultz, P. G. Functionalized Xenon as a Biosensor. *Proc. Natl. Acad. Sci. U. S. A.* **2001**, *98* (19), 10654–10657.

(13) Palaniappan, K. K.; Ramirez, R. M.; Bajaj, V. S.; Wemmer, D. E.; Pines, A.; Francis, M. B. Molecular Imaging of Cancer Cells Using a Bacteriophage-Based (129) Xe NMR Biosensor. *Angew. Chem. Int. Ed. Engl.* **2013**, *112*, 1–6.

(14) Slack, C. C.; Finbloom, J. A.; Jeong, K.; Bruns, C. J.; Wemmer, D. E.; Pines, A.; Francis, M. B. Rotaxane Probes for Protease Detection by ^{129} Xe HyperCEST NMR. *Chem. Commun.* **2017**, *53* (6), 1076–1079.

(15) Wang, Y.; Dmochowski, I. J. Cucurbit[6]Uril Is an Ultrasensitive ^{129} Xe NMR Contrast Agent. *Chem. Commun.* **2015**, *51* (43), 8982–8985.

(16) Barrow, S. J.; Kasera, S.; Rowland, M. J.; del Barrio, J.; Scherman, O. A. Cucurbituril-Based Molecular Recognition. *Chem. Rev.* **2015**, *115* (22), 12320–12406.

(17) Kim, B. S.; Ko, Y. H.; Kim, Y.; Lee, H. J.;

Selvapalam, N.; Lee, H. C.; Kim, K. Water Soluble Cucurbit[6]Uril Derivative as a Potential Xe Carrier for ^{129}Xe NMR-Based Biosensors. *Chem. Commun.* **2008**, *0* (24), 2756.

(18) Hane, F. T.; Li, T.; Smylie, P.; Pellizzari, R. M.; Plata, J. A.; DeBoef, B.; Albert, M. S. In Vivo Detection of Cucurbit[6]Uril, a Hyperpolarized Xenon Contrast Agent for a Xenon Magnetic Resonance Imaging Biosensor. *Sci. Rep.* **2017**, *7* (1), 41027.

(19) Bruns, C. J.; Stoddart, J. F. *The Nature of the Mechanical Bond : From Molecules to Machines*.

(20) Bruns, C. J.; Stoddart, J. F. Rotaxane-Based Molecular Muscles. *Acc. Chem. Res.* **2014**, *47* (7), 2186–2199.

(21) Finbloom, J. A.; Slack, C. C.; Bruns, C. J.; Jeong, K.; Wemmer, D. E.; Pines, A.; Francis, M. B.; Shen, C.; New, E. J.; Major, J. L.; et al. Rotaxane-Mediated Suppression and Activation of Cucurbit[6]Uril for Molecular Detection by ^{129} Xe HyperCEST NMR. *Chem. Commun.* **2016**, *52* (15), 3119–3122.

(22) Wang, Y.; Roose, B. W.; Philbin, J. P.; Doman, J. L.; Dmochowski, I. J. Programming A Molecular Relay for Ultrasensitive Biodetection through (129) Xe NMR. *Angew. Chem. Int. Ed. Engl.* **2016**, *55* (5), 1733–1736.

(23) Truxal, A. E.; Cao, L.; Isaacs, L.; Wemmer, D. E.; Pines, A. Directly Functionalized Cucurbit[7]Uril as a Biosensor for the Selective Detection of Protein Interactions by ^{129} Xe HyperCEST NMR. *Chem. – A Eur. J.* **2019**, chem.201900610.

(24) Hane, F. T.; Fernando, A.; Prete, B. R. J.; Peloquin, B.; Karas, S.; Chaudhuri, S.; Chahal, S.; Shepelytskyi, Y.; Wade, A.; Li, T.; et al. Cyclodextrin-Based Pseudorotaxanes: Easily Conjugatable Scaffolds for Synthesizing Hyperpolarized Xenon-129 Magnetic Resonance Imaging Agents. *ACS Omega* **2018**, *3* (1), 677–681.

(25) Szatrowski, T. P.; Nathan, C. F. Production of Large Amounts of Hydrogen Peroxide by Human Tumor Cells. *Cancer Res.* **1991**, *51* (3), 794–798.

(26) Houstis, N.; Rosen, E. D.; Lander, E. S. Reactive Oxygen Species Have a Causal Role in Multiple Forms of Insulin Resistance. *Nature* **2006**, *440* (7086), 944–948.

(27) Niethammer, P.; Grabher, C.; Look, A. T.; Mitchison, T. J. A Tissue-Scale Gradient of Hydrogen Peroxide Mediates Rapid Wound Detection in Zebrafish. *Nature* **2009**, *459* (7249), 996–999.

(28) Reuter, S.; Gupta, S. C.; Chaturvedi, M. M.; Aggarwal, B. B. Oxidative Stress, Inflammation, and Cancer: How Are They Linked? *Free Radic. Biol. Med.* **2010**, *49* (11), 1603–1616.

(29) Weinstain, R.; Savariar, E. N.; Felsen, C. N.; Tsien, R. Y. In Vivo Targeting of Hydrogen Peroxide by Activatable Cell-Penetrating Peptides. *J. Am. Chem. Soc.* **2014**, *136* (3), 874–877.

(30) Nowak, D.; Kasielski, M.; Antczak, A.; Pietras, T.; Bialasiewicz, P. Increased Content of Thiobarbituirc Acid Reactive Substances and Hydrogen Peroxide in the Expired Breath Condensate of Patients with Stable Chronic Obstructive Pulmonary Disease: No Significant Effect of Cigarette Smoking. *Respir. Med.* **1999**, *93* (6), 389–396.

(31) Majewska, E.; Kasielski, M.; Luczynski, R.; Bartosz, G.; Bialasiewicz, P.; Nowak, D. Elevated Exhalation of Hydrogen Peroxide and Thiobarbituric Acid Reactive Substances in Patients with Community Acquired Pneumonia. *Respir. Med.* **2004**, *98* (7), 669–676.

(32) Muller, F. L.; Song, W.; Jang, Y. C.; Liu, Y.; Sabia, M.; Richardson, A.; Van Remmen, H. Denervation-Induced Skeletal Muscle Atrophy Is Associated with Increased Mitochondrial ROS Production. *Am. J. Physiol. Regul. Integr. Comp. Physiol.* **2007**, *293* (3), R1159–R1168.

(33) Lee, D.; Khaja, S.; Velasquez-Castano, J. C.; Dasari, M.; Sun, C.; Petros, J.; Taylor, W. R.; Murthy, N. In Vivo Imaging of Hydrogen Peroxide with Chemiluminescent Nanoparticles. *Nat. Mater.* **2007**, *6* (10), 765–769.

(34) Van de Bittner, G. C.; Dubikovskaya, E. A.; Bertozzi, C. R.; Chang, C. J. In Vivo Imaging of Hydrogen Peroxide Production in a Murine Tumor Model with a Chemoselective Bioluminescent Reporter. *Proc. Natl. Acad. Sci. U. S. A.* **2010**, *107* (50), 21316–21321.

(35) Srikun, D.; Miller, E. W.; Domaille, D. W.; Chang, C. J. An ICT-Based Approach to Ratiometric Fluorescence Imaging of Hydrogen Peroxide Produced in Living Cells. *J. Am. Chem. Soc.* **2008**, *130* (14), 4596–4597.

(36) Carroll, V.; Michel, B. W.; Blecha, J.; VanBrocklin, H.; Keshari, K.; Wilson, D.; Chang, C. J. A Boronate-Caged [^{18} F]FLT Probe for Hydrogen Peroxide Detection Using Positron Emission Tomography. *J. Am. Chem. Soc.* **2014**, *136* (42), 14742–14745.

(37) Lin, V. S.; Dickinson, B. C.; Chang, C. J. Boronate-Based Fluorescent Probes: Imaging Hydrogen Peroxide in Living Systems. *Methods Enzymol.* **2013**, *526*.

(38) Nikolaou, P.; Coffey, A. M.; Walkup, L. L.; Gust, B. M.; Whiting, N.; Newton, H.; Barcus, S.; Muradyan, I.; Dabaghyan, M.; Moroz, G. D.; et al. Near-Unity Nuclear Polarization with an Open-Source ^{129}Xe Hyperpolarizer for NMR and MRI. *Proc. Natl. Acad. Sci.* **2013**, *110* (35), 14150 LP-14155.

(39) Meschke, C.; Buschmann, H. J.; Schollmeyer, E. Complexes of Cucurbituril with Alkyl Mono- and Diammonium Ions in Aqueous Formic Acid Studied by Calorimetric Titrations. *Thermochim. Acta* **1997**,

297 (1–2), 43–48.

(40) Buschmann, H. J.; Mutihac, L.; Mutihac, R. C.; Schollmeyer, E. Complexation Behavior of Cucurbit[6]Uril with Short Polypeptides. *Thermochim. Acta* **2005**, *430* (1–2), 79–82.

(41) Danylyuk, O.; Fedin, V. P.; Sashuk, V. Kinetic Trapping of the Host-Guest Association Intermediate and Its Transformation into a Thermodynamic Inclusion Complex. *Chem. Commun.* **2013**, *49* (18), 1859–1861.

(42) Chen, Y.; Molnár, M.; Li, L.; Friberg, P.; Gan, L.-M.; Brismar, H.; Fu, Y. Characterization of VCAM-1-Binding Peptide-Functionalized Quantum Dots for Molecular Imaging of Inflamed Endothelium. *PLoS One* **2013**, *8* (12), e83805.

(43) Schlesinger, M.; Bendas, G. Vascular Cell Adhesion Molecule-1 (VCAM-1)-An Increasing Insight into Its Role in Tumorigenicity and Metastasis. *Int. J. Cancer* **2015**, *136* (11), 2504–2514.

(44) Finbloom, J. A.; Han, K.; Aanei, I. L.; Hartman, E. C.; Finley, D. T.; Dedeo, M. T.; Fishman, M.; Downing, K. H.; Francis, M. B. Stable Disk Assemblies of a Tobacco Mosaic Virus Mutant as Nanoscale Scaffolds for Applications in Drug Delivery. *Bioconjug. Chem.* **2016**, *27* (10), 2480–2485.

(45) Finbloom, J.; Aanei, I.; Bernard, J.; Klass, S.; Elledge, S.; Han, K.; Ozawa, T.; Nicolaides, T.; Berger, M.; Francis, M. Evaluation of Three Morphologically Distinct Virus-Like Particles as Nanocarriers for Convection-Enhanced Drug Delivery to Glioblastoma. *Nanomaterials* **2018**, *8* (12), 1007.

(46) Adriani, G.; de Tullio, M. D.; Ferrari, M.; Hussain, F.; Pascazio, G.; Liu, X.; Decuzzi, P. The Preferential Targeting of the Diseased Microvasculature by Disk-like Particles. *Biomaterials* **2012**, *33* (22), 5504–5513.

(47) Dixon, S. J.; Stockwell, B. R. The Role of Iron and Reactive Oxygen Species in Cell Death. *Nat. Chem. Biol.* **2014**, *10* (1), 9–17.

(48) Martinez-Outschoorn, U. E.; Lin, Z.; Trimmer, C.; Flomenberg, N.; Wang, C.; Pavlides, S.; Pestell, R. G.; Howell, A.; Sotgia, F.; Lisanti, M. P. Cancer Cells Metabolically "Fertilize" the Tumor Microenvironment with Hydrogen Peroxide, Driving the Warburg Effect: Implications for PET Imaging of Human Tumors. *Cell Cycle* **2011**, *10* (15), 2504–2520.

Entry for the Table of Contents

COMMUNICATION

The CB6 molecule can host single ^{129}Xe atoms in its interior cavity, creating a distinct chemical environment that can be observed by ^{129}Xe hyperCEST NMR. To create a “turn on” probe, CB6 can be threaded onto a molecular axle and capped by two stoppers to prevent the entry of ^{129}Xe into the CB6 interior. Selective cleavage of one stopper group by H_2O_2 releases CB6, producing a hyperCEST response.

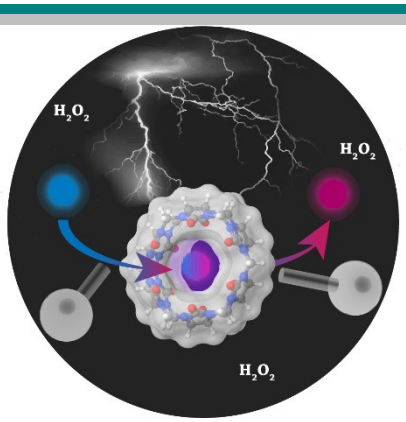

Sarah H. Klass, Ashley E. Truxal, Tahoe A. Fiala, Joseph Kelly, Dang Nguyen, Joel A. Finbloom, David E. Wemmer, Alexander Pines, Matthew B. Francis

Page No. – Page No.

Rotaxane probes for the detection of hydrogen peroxide by ^{129}Xe hyperCEST NMR